Development of a regional GPS-based ionospheric TEC model for South Africa

Ben D.L. Opperman, Pierre J. Cilliers, Lee-Anne McKinnell and Ray Haggard

Abstract

Advances in South African space physics research and related disciplines require better spatial and time resolution ionospheric information than was previously possible with the existing ionosonde network. A GPS-based, variable degree adjusted spherical harmonic (ASHA) model was developed for near real-time regional ionospheric total electron content (TEC) mapping over South Africa. Slant TEC values along oblique GPS signal paths are quantified from a network of GPS receivers and converted to vertical TEC by means of the single layer mapping function. The ASHA model coefficients and GPS differential biases are estimated from vertical TEC at the ionospheric pierce points and used to interpolate TEC at any location within the region of interest. Diurnal TEC variations with one minute time resolution and time-varying 2D regional TEC maps are constructed. In order to validate the ASHA method, simulations with an IRI ionosphere were performed, while the ASHA results from actual data were compared with two independent GPS-based methodologies and measured ionosonde data.

1. Objective

The study objective was to develop a regional GPS-based, bias-free ionospheric TEC mapping methodology for South Africa which would provider a better resolution in time and space than is currently available by means of the limited number of ionosondes and International GNSS Service (IGS) GPS receivers in South Africa.

2. Introduction

The ionosphere is the region of ionised plasma extending 80–1200 km above the Earth's surface and forms the transition region between the neutral atmosphere and the fully ionized magnetospheric plasma (Baumjohann and Treumann, 1999). Free electrons and ions are produced during interaction of extreme ultra violet (EUV) and X-ray radiation with upper atmosphere neutral gas. Ionospheric activity is subject to regular diurnal, seasonal, and solar cycle variation as well as irregular geomagnetic activity caused by solar storms, travelling ionospheric disturbances, and scintillation. Diurnal electron density peaks at two hours past local noon, and solar cycle variation during increased sunspot activity associated with 11 year solar variations. The ionosphere is structured in different regions (Hargreaves, 1992). The D-

layer (<90 km), E-layer (peaks at 105 km), F_1 (peaks 160–180 km) and the F_2 layer (peaks 200–600 km). During nighttime, the D- and E-layers disappear and the F_1 and F_2 layers combine to form the F layer. The maximum electron density occurs in the F_2 layer.

The ionosphere significantly affects terrestrial-based radio communication and attenuates high frequency wave propagating through it. Its effect on radio waves of astronomical origin in the bandwidth 70 MHz to 20 GHz includes phase delay, phase jitter, attenuation, refraction, scintillation, and Faraday rotation, a left polarised rotation. These phenomena are proportional to the total electron content (TEC) of the plasma along the signal path. Ionospheric errors on signals received from GPS satellites signals constitute the largest contributor to errors in position fix by single-frequency GPS receivers. These phenomena are more pronounced during periods of severe solar activity such as geomagnetic storms. The Satellite Based Augmentation Systems (SBAS) such as the American Wide Area Augmentation System (WAAS) and the European Geostationary Navigation Overlay Service (EGNOS) have, in part, been developed to supply near real-time ionospheric correction parameters to GPS users for precision navigation and surveying applications (Hofmann-Wellenhof et al., 2001).

3. Conventional ionospheric measurements over South Africa

Vertical electron density profiles are measured at 30 min intervals with three Lowell DPS ionosondes located, respectively, at Grahamstown, Eastern Cape (26.53°E, 33.30°S), Louisvale, Northern Cape (21.20°E, 28.50°S), and Madimbo, Limpopo (30.90°E, 22.40°S). South African ionosonde data are archived at (SPIDR). These observations presently constitute the only operational measurements of the ionosphere over South Africa (Fig. 1). An ionospheric sounding constitutes a vertical sweep of the ionosphere by a pre-determined frequency band (<30 MHz). During a sounding electron density values are calculated from reflected radio waves corresponding to the density-dependent critical plasma frequency, f_p, of the ionised plasma, and density heights are inferred from the time-delay of the reflected radio wave. The relation between the electron density, N_e, and density-dependent plasma frequency, f_p is given by (e.g., Chen, 1984).

$$N_e = \frac{m(2\pi f)^2 \varepsilon_0}{e^2} \quad (1)$$

where N_e, electron density (number electrons/m^3); f, reflected radio frequency (Hz). $f = f_p$, e, m is the electron charge and mass, respectively, (1.6022×10^{-19} C, 9.1095×10^{-31} kg); ε_0, is the vacuum permittivity (8.854×10^{-12} F m^{-1}).

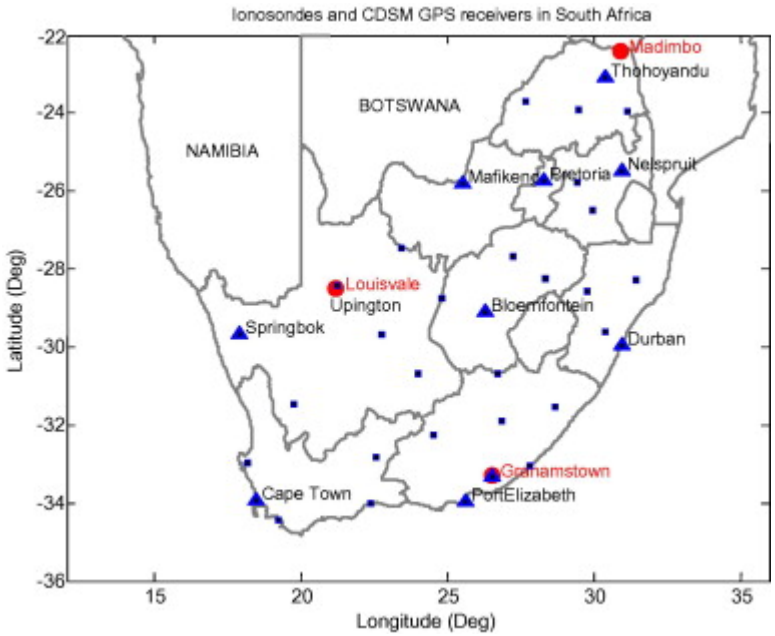

Fig. 1. Distribution of ionosondes and CDSM GPS network. The triangles represent real-time GPS receivers, and squares off-line (06h00–18h00) GPS receivers. Circles represent ionosonde sounders. Ionosondes and GPS receivers are, respectively, spaced approximately 1000 and 250 km apart.

The calculated electron densities and associated heights constitute an electron density profile of the bottom side ionosphere up to the F_2 peak density height (*hmF2*) (Fig. 2). Signals above the F_2 peak density frequency (*foF2*) are transmitted through the ionosphere. Topside profiles are extrapolated using a Chapman function with a scale height derived from the shape of the bottomside profile near the F2 peak (Reinisch et al., 2004).

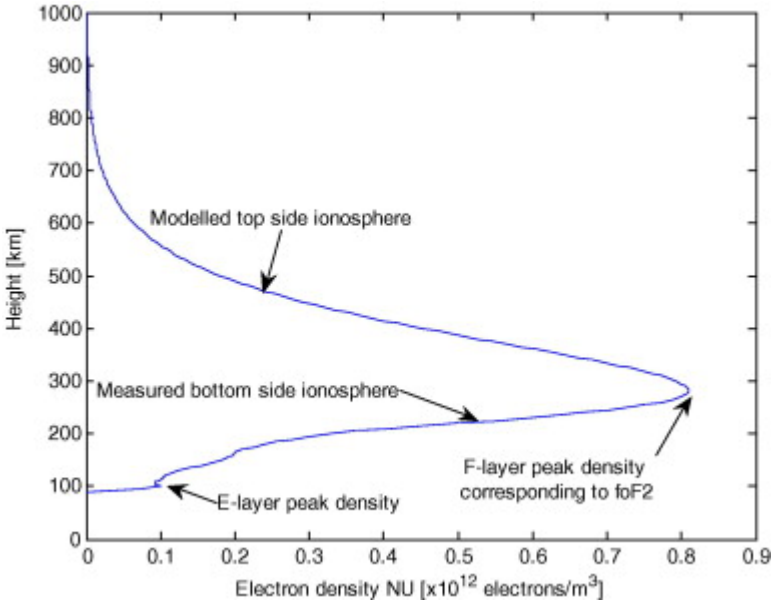

Fig. 2. A typical profile of electron density vs. height as obtained from ionosonde data. The specific profile pertains to 2005.01.31, 14:30 UT as recorded at the Grahamstown ionosonde. The bottom side profile (below the peak electron density value) is derived from a measured ionogram, while the topside profile is obtained by fitting a Chapman model to the peak electron density value. The total electron content (TEC) is obtained by integration of the density along the vertical height coordinate. For this profile the TEC was determined to be 19.6 TECU.

Advances in space physics research, radio astronomy, radio communications, and precision navigation all depend on an accurate characterization of the ionosphere. These applications require higher spatial and temporal ionospheric information than is presently feasible with the existing ionosonde network. To supplement and improve the spatial resolution of existing ionospheric observations, measurements from GPS signals from the South African network of GPS receivers managed by the Chief Directorate Surveys and Mapping (CDSM) are being investigated.

4. TEC from global positioning system (GPS)

A radio signal propagating through the ionosphere experiences a group delay and phase advance due to the ionosphere's dispersive nature. This delay/advance is proportional to the total electron content (TEC) along the signal path and inversely proportional to the square of the carrier frequency and given, to first order, by (Hofmann-Wellenhof et al., 2001)

$$\Delta_{\mathrm{ph}}^{\mathrm{iono}} = -\frac{40.28}{f^2}\mathrm{TEC} \quad \text{and} \quad \Delta_{\mathrm{gr}}^{\mathrm{iono}} = \frac{40.28}{f^2}\mathrm{TEC} \tag{2}$$

TEC is quantified from GPS measurements by a linear combination of the measured pseudo range and phase observables registered by the receiver on two carrier frequencies (f_1 = 1.5754 × 10^9 Hz and f_2 = 1.2276 × 10^9 Hz). TEC is measured in TEC units with 1 TECU = 10^{16} e m^{-2}. Measured pseudo range (P), constitute a combination of the geometric range, (ρ), speed of light in a vacuum (c), ionospheric range error ($\Delta\rho_{\mathrm{ion}}$), tropospheric range error ($\Delta\rho_{\mathrm{trop}}$), satellite and receiver biases, b_S and b_R, multipath and other errors (ε):

$$P = \rho + \Delta\rho_{\mathrm{ion}} + \Delta\rho_{\mathrm{trop}} + c(\Delta t_c^S - \Delta t_c^R) + c(b_S + b_R) + \varepsilon \tag{3}$$

Likewise the measured phase can be expressed as

$$L = \rho - \Delta\rho_{\mathrm{ion}} + \Delta\rho_{\mathrm{trop}} + c(\Delta t_c^R - \Delta t_c^S) + \lambda B + \mathrm{E} \tag{4}$$

where λ is the carrier wavelength and B an unknown integer ambiguity offset.

Code-based TEC is calculated from the difference between the two observed pseudo ranges (Schaer, 1999)

$$P_4 = P_2 - P_1 = \left(\frac{1}{f_2^2} - \frac{1}{f_1^2}\right) \cdot \alpha \cdot \mathrm{TEC_P}, \alpha = 40.3 \times 10^{16} \quad (5)$$

and

$$L_4 = L_1 \frac{c}{f_1} - L_2 \frac{c}{f_2} = \left(\frac{1}{f_2^2} - \frac{1}{f_1^2}\right) \cdot \alpha \cdot \mathrm{TEC_L} \quad (6)$$

Code-based TEC (TEC_P) is noisier than phase-based TEC (TEC_L), largely due to multipath, but the latter suffers an unknown integer ambiguity offset and is subject to cycle slips associated with rapid ionospheric scintillations. Corrected TEC_L is obtained from TEC_P by means of a “levelling” process by which continuous sections of TEC_L are adjusted to the mean of corresponding sections of TEC_P. The resultant product is the GPS-derived slant TEC along the signal path between satellite and receiver.

Slant TEC (STEC) calculated along oblique signal paths are mapped to vertical TEC (VTEC) values by means of the Single Layer Model (SLM). The mapping is accomplished employing a cosec transform (Schaer, 1999)

$$\mathrm{STEC} = \frac{\mathrm{VTEC}}{\cos z'}, \quad \sin z' = \frac{R_e}{R_e + H} \sin z \quad (7)$$

with

z is the satellite zenith angle, R_e is the Earth equatorial radius (6378.134 km), H is assumed SLM height (350 km).

5. GPS infrastructure

The Chief Directorate Surveys and Mapping (CDSM) operates a network of approximately, fourty geodetic grade dual frequency Ashtech GPS receivers (Fig. 1). Seventeen receiver stations in the grid stream 1 Hz sampled data in real-time to Cape Town and the remaining receivers upload 1 Hz data recorded between 06h00 and 18h00 offline. All data is processed and archived in Cape Town and is available via ftp server (TRIGNET) in Receiver Independent Exchange (RINEX) format.

6. GPS methodologies and products

Several methodologies exist for integrating slant TEC from multiple receiver-satellite combinations to render optimal vertical TEC at desired locations and estimate instrumental (differential code) biases not calculated in Eqs. (5), (6) and (7). The two methodologies used for comparative purposes in this case study, respectively, employ computerised ionospheric tomography (CIT) and spherical harmonic analysis (SHA). CIT permits a 3D reconstruction of ionospheric electron densities, compared to the 2D TEC – only estimation by SHA. SHA, however, is a relative simple algorithm to employ and can render TEC estimate at time scales of seconds, compared to CIT, which requires relative long data integration periods to contain ill-conditioning and render results at 15–30 min intervals. The ASHA methodology presented in this paper is a spherical harmonic model based on that developed for regional ionospheric *foF2* mapping in Europe (De Franceschi et al., 1994).

6.1. Multi-Instrument Data Analysis System (MIDAS)

The MIDAS system, developed by the University of Bath, uses slant TEC derived from GPS differential phase to invert the 4D (lon, lat, altitude, and time) ionisation distribution in the ionosphere as electron density values contained in volume elements (voxels) (Mitchell and Spencer, 2003). MIDAS has been extensively tested against ionosonde and incoherent scatter radar data, making it a well suited for this comparative study. For this study, the vertical TEC at an ionosonde location is derived by vertically integrating through the CIT-inverted electron density distribution constituting an electron density profile. The relative long (30–60 min) data integration period of MIDAS, however, does not permit high time resolution TEC mapping.

6.2. Global ionosphere maps (GIM)

Global ionosphere maps (GIM) are generated on a daily basis at the Center for Orbit Determination in Europe (CODE) using data from about 150 IGS and other institutions' GPS receivers. The VTEC is modelled in a solar-geomagnetic reference frame using a spherical harmonics expansion up to degree and order 15. The temporal resolution is two-hours and spatial resolution of 5.0° and 2.5° in longitude and latitude, respectively. Instrumental biases for all GPS satellites and ground stations are estimated as constant values for each day. The parameters required to represent the global VTEC distribution are distributed in the IONEX format.

7. Adjusted spherical harmonic model (ASHA)

The new ASHA model introduced in this paper is based on the Global Spherical Harmonic Analysis (GSHA) methodology used by Center for Orbit Determination in Europe (CODE) (Schaer, 1999). The objective of developing the new model is twofold: (1) Improve the time and spatial resolution of regional TEC maps currently available for South Africa from (CODE) (desired: 5–10 min on a 0.5° × 0.5° grid), and (2) investigate the feasibility of estimating near real-time TEC from observations by a relative dense network of regional GPS receivers.

Both estimation approaches model TEC as a spherical harmonic expansion Eq. (8) using observed ionospheric delays along oblique ray paths and employing a single layer mapping (SLM) function to map calculated slant TEC to vertical TEC at sub ionospheric pierce points (IPP). The major difference between ASHA and GSHA is briefly discussed. GSHA and ASHA both model TEC as a spherical harmonic expansion:

$$\mathrm{TEC}(\lambda,\phi) = \sum_{n=0}^{N}\sum_{m=0}^{n} \overline{P}_{nm}[\cos(\phi)]\{a_{nm}\sin(m\lambda) + b_{nm}\cos(m\lambda)\} \quad (8)$$

λ, IPP Sun-fixed longitude ∈[0°, 360°]; ϕ, IPP co-latitude ∈[0°, 180°]; $\overline{P}_{nm}$, normalized associated Legendre functions; a_{nm}, b_{nm}, desired SHM coefficients and; n,m, degree and order of SHM expansion

ASHA and the GSHA both utilise the Sun-fixed longitude of the IPP, i.e. the longitude of the IPP expressed relative to the Sun's mean geographic longitude. Sun-fixed longitude conveniently encapsulates the IPPs time and longitudinal parameters in a single angular observation spanning 360° over a 24 h revolution. The co-latitude of the IPP, i.e. the polar angle measured from the North Pole, however, is handled differently by the two approaches.

In the GSHA methodology, no change to the co-latitude is required as the n wavelengths of the Legendre polynomial are defined over the 180° latitude span of a sphere, which is sufficiently covered by IPP observations defined by the IGS global receiver network geometry (∼175° latitude span). The latitudinal span of IPPs from the South African regional GPS network, however, is approximately 30°, which maps the regionally confined IPPs onto a relative narrow latitude band on a sphere when combined with the Sun-fixed longitude. To fit the same number of latitude wavelengths in this relative narrow latitude band will require a significantly higher degree SH expansion when using the conventional GSHA.

ASHA employs a similar approach to (De Santis et al., 1991) by translating and scaling the narrow co-latitude band of the IPPs to a hemisphere using the minimum co-latitude of the IPPs, ϕ_0 and the latitude span, θ, of the observations:

$$\phi' - \frac{90^\circ}{\theta} \cdot (\phi - \phi_0) \tag{9}$$

The IPP co-latitude in Eq. (8) is subsequently replaced by the scaled co-latitude, ϕ', defined on a hemisphere [0°, +90°]. This transformation is valid as the Legendre polynomials form a set of orthogonal functions on [0°, 180°], but may be used as two sets of orthogonal functions in [0°, +90°] to fit any general functions defined in this interval (De Santis, 1992). The ASHA algorithm is briefly outlined.

Define the parameter

$$\mu = \frac{40.28}{cf_1^2} \tag{10}$$

The ionospheric time-delay, $\Delta\tau_{\text{ion}}$, is defined from Eqs. (2) and (10)

$$\Delta\tau_{\text{ion}} = \mu \cdot \text{TEC} \tag{11}$$

The slant ionospheric delay (including interfrequency differential biases b_R, b_S) follows from Eqs. (3), (4), (5), (6) and (7)

$$\begin{aligned} \Delta\tau_{\text{ion}} &= \mu \cdot \frac{\text{VTEC}}{\cos z'} + (b_R - b_S) \\ &= \mu\gamma \cdot \text{VTEC} + (b_R - b_S) \end{aligned} \tag{12}$$

Separate the SHM representation of the VTEC

$$\begin{aligned} \text{VTEC}(\lambda, \phi) = \sum_{n=0}^{N} \sum_{m=0}^{n} \overline{P}_{nm}[\cos(\phi)]\{a_{nm}\sin(m\lambda) \\ + b_{nm}\cos(m\lambda)\} \end{aligned} \tag{13}$$

into

$$\begin{aligned} \text{VTEC}(\lambda, \phi) = \sum_{n=0}^{N} \sum_{m=0}^{n} \overline{P}_{nm}[\cos(\phi)] \cdot a_{nm}\sin(m\lambda) \\ + \sum_{n=0}^{N} \sum_{m=0}^{n} \overline{P}_{nm}[\cos(\phi)] \cdot b_{nm}\cos(m\lambda) \end{aligned} \tag{14}$$

and substitute into Eq. 12

$$\Delta\tau_{\text{ion}} = \mu\gamma \cdot \left(\sum_{n=0}^{N} \sum_{m=0}^{n} \overline{P}_{nm}[\cos(\phi)] \cdot a_{nm} \sin(m\lambda) + \sum_{n=0}^{N} \sum_{m=0}^{n} \overline{P}_{nm}[\cos(\phi)] \cdot b_{nm} \cos(m\lambda) \right) + (b_R - b_S) \tag{15}$$

The unknown coefficients a_{nm}, b_{nm} and interfrequency biases b_R, b_S are estimated by means of a weighted least squares method. The Jacobian for the least squares model is obtained by taking the partial derivatives of the measurements, $\Delta\tau_{\text{ion}}$ w.r.t. the unknowns:

$$\begin{aligned} \frac{\partial \Delta\tau_{ion}}{\partial a_{nm}} &= \mu\gamma \sum \sum \overline{P}_{nm}[\cos\phi] \cdot \cos(m\lambda) \\ \frac{\partial \Delta\tau_{ion}}{\partial b_{nm}} &= \mu\gamma \sum \sum \overline{P}_{nm}[\cos\phi] \cdot \sin(m\lambda) \\ \frac{\partial \Delta\tau_{ion}}{\partial b_R} &= +1 \end{aligned} \tag{16}$$

$$\frac{\partial \Delta\tau_{ion}}{\partial b_S} = -1$$

8. Methodology

The software implementation of the ASHA algorithm was tested using slant TEC observations simulated from the IRI2001 (Bilitza, 2001) model and comparing the diurnal vertical TEC profile, interpolated from the estimated coefficients, with a reference diurnal IRI-vertical TEC profile. Simulated slant TEC observations, calculated in 60 s intervals along actual GPS satellite signal paths observed over a 24 h period for 5 May 2005 and a reference diurnal vertical TEC profile calculated in 60 s interval for the same period, were used for the investigation. The effects of using different SHM degrees and different number of receivers for interpolating the profile were also investigated by comparing results reconstructed from coefficients estimated from 12-degree to 15-degree models for each of two simulation data sets: (1) data from a single receiver (Grahamstown) and (2) data from eight receivers (Table 1). The results from the simulation study are presented in Fig. 3.

Table 1.

GPS receivers used in study. 5 May 2005

Receiver	Location (long, lat)
Bloemfontein	26.30, −29.10
Durban	30.95, −29.97
Cape Town	18.47, −33.95
Grahamstown	26.50, −33.32
Mafikeng	25.54, −25.81
Nelspruit	30.98, −25.48
Thohoyandou	30.38, −23.10
Pretoria	28.28, −25.73
Upington	21.26, −28.41
Springbok	17.88, −29.67

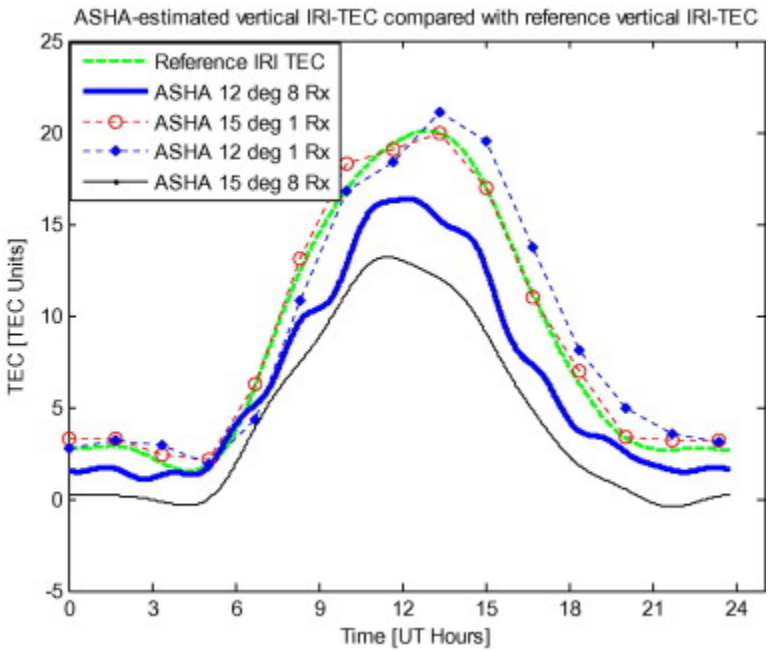

Fig. 3. Comparison of diurnal IRI-TEC variation values at Grahamstown estimated from IRI-simulated data along signals paths from, respectively, one receiver at Grahamstown and eight GPS receivers distributed over South Africa. The (green) broken line represents reference vertical TEC values calculated from the IRI2001 model. The ASHA-TEC values were interpolated from, respectively, 12-degree ASHA coefficients estimated from eight receivers' data (solid blue line), 12-degree single receiver data (broken blue diamonds), 15-degree coefficients estimated from eight receivers' data (thin black line) and 15-degree single receiver

data (broken red circle). Time interval is one minute. (For interpretation of the references to color in this figure legend, the reader is referred to the web version of this paper.)

ASHA was subsequently applied to GPS measurements from receivers listed in Table 1. (RINEX) observation files for 5 May 2005, sampled at 60 s and satellite orbital position files from (IGS) were used for the investigation and a 15° elevation cut-off angle was employed to minimise multipath errors. Twelve-degree coefficients were estimated at Grahamstown, Louisvale, and Madimbo using observations from eight receivers listed in Table 1 (limited computer resources and un-optimised code prevented higher degree coefficient estimation at the time). For Grahamstown and Louisvale, the Thohoyandou receiver was ignored and for Madimbo, the Cape Town receiver was ignored.

To investigate the performance of single receiver higher order solutions, individual 15-degree solutions were obtained for observations from each of the GPS receivers at Grahamstown, Upington and Thohoyandou, which are in close proximity of the ionosondes. The Upington and Thohoyandou receivers are, respectively, located 17 and 95 km from Louisvale and Madimbo receivers, and the Grahamstown GPS receiver and ionosonde are co-located.

Diurnal vertical TEC profiles were interpolated at one minute intervals at Grahamstown, Louisvale, and Madimbo using the 15-degree individual solutions and the 12-degree multi-receiver solutions. Diurnal TEC profiles for these locations were also calculated from MIDAS and GIM for the same day. In addition, TEC was calculated from hand-scaled ionograms measured at Grahamstown and Louisvale. No Madimbo ionosonde data were available for the day. ASHA-estimated diurnal TEC profiles at the three locations were compared to MIDAS, GIM and ionosonde measurements. The results from this investigation are presented in Fig. 4a–d. Two-dimensional TEC maps were constructed from the estimated coefficients by interpolating over a 0.5° × 0.5° grid (Fig. 5).

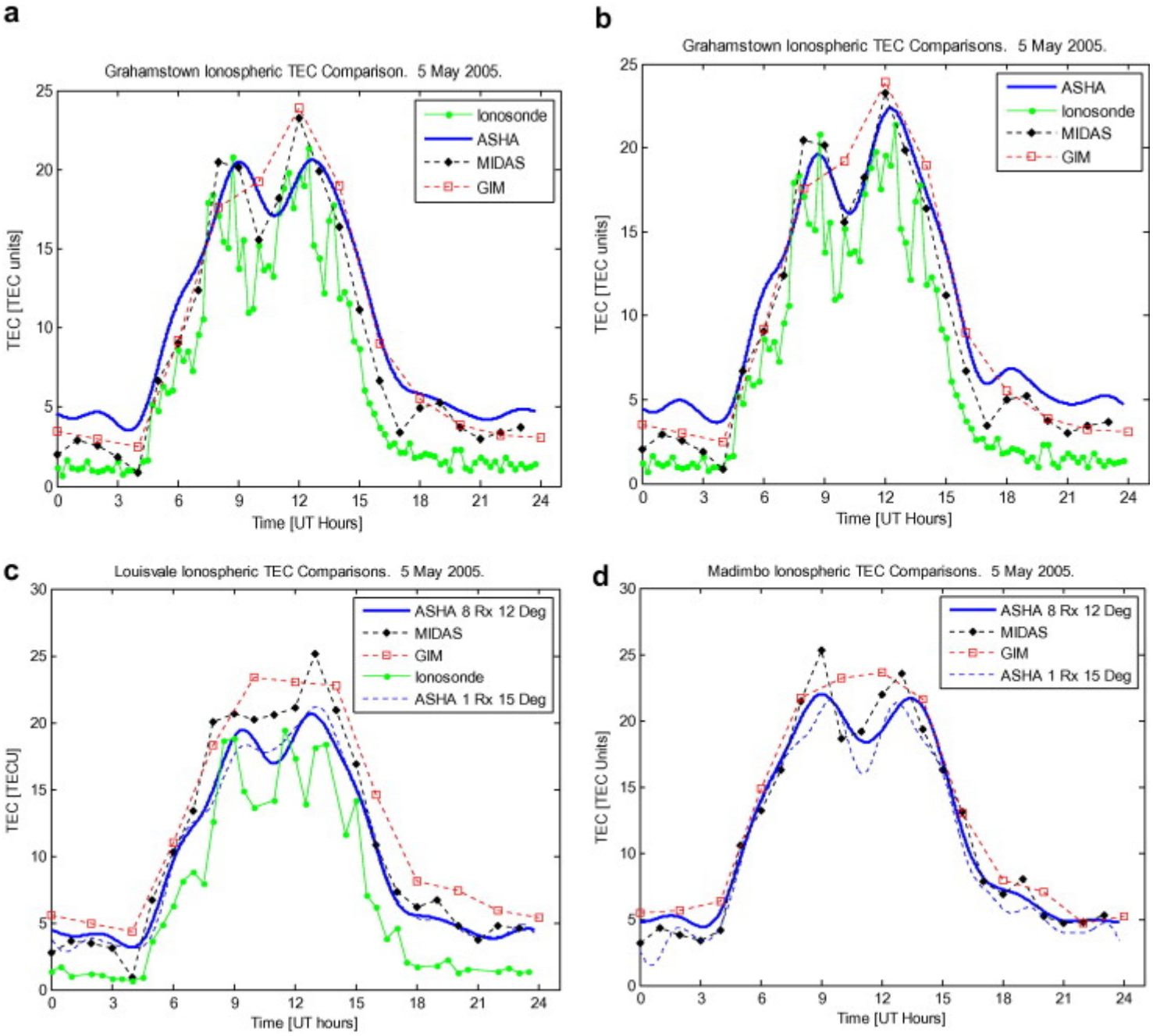

Fig. 4. (a–d) Comparison of diurnal GPS-derived Ionospheric TEC variation values interpolated from 12-degree to 15-degree ASHA coefficients estimated, respectively, from eight and individual CDSM GPS receivers distributed over South Africa. The time interval for ASHA, MIDAS and GIM results are, respectively, one minute, one hour and two-hours. Ionosonde measurements are at 30 min intervals. (a) Ionospheric vertical TEC comparisons: Grahamstown. The 12-degree ASHA solution obtained from eight GPS receivers distributed over South Africa. (b) Comparison of diurnal Ionospheric TEC variation values interpolated from 15-degree ASHA coefficients estimated from a single GPS receiver co-located with Grahamstown Ionosonde (broken line). (c) Ionospheric vertical TEC comparisons: Louisvale. The 12-degree and 15-degree ASHA solutions are, respectively, obtained using observations

from eight GPS receivers and one GPS receiver (Upington). (d) Ionospheric vertical TEC comparisons: Madimbo. The 12-degree and 15-degree ASHA solutions are, respectively, obtained using observations from eight GPS receivers and one GPS receiver (Thoyoyandou). No ionosonde data were available for this day.

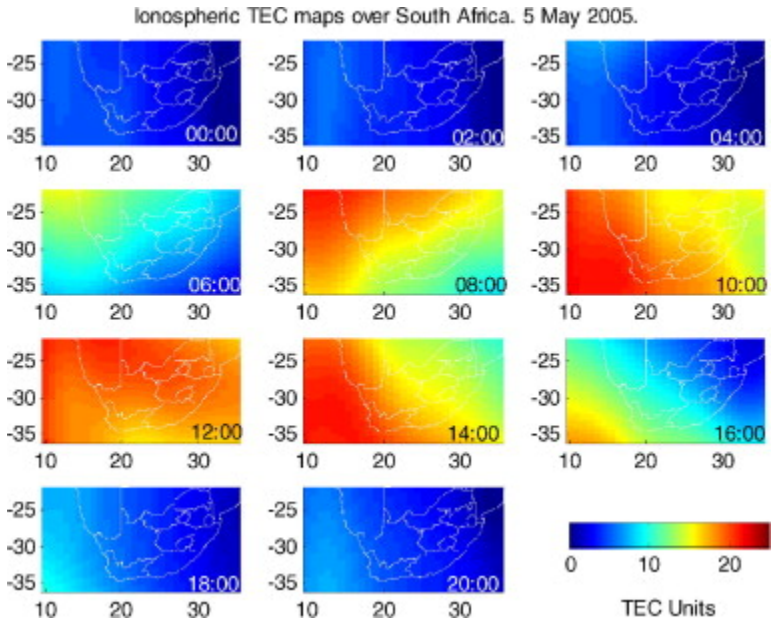

Fig. 5. TEC maps interpolated from a 12-degree ASHA solution on a 0.5° × 0.5° grid. Time is in UT. TEC maps with higher time and spatial resolution may be constructed from the same coefficient set.

The ASHA algorithm was implemented in Matlab® (Mathworks) on a 3.2 GHz PC with 2 GB RAM using 60-second interval GPS (RINEX) observation files for 5 May 2005 (Table 1). The ASHA code, respectively, processed data from one and eight receivers in 2.3 and in 15 min.

9. Discussion

Given the known limitations of IRI over Southern Africa, a qualitative comparison is discussed for the simulation results. The ASHA-IRI interpolated results (Fig. 3) follow expected diurnal TEC variations with low nighttime TEC values and midday peaks and displayed no negative TEC values. It appears that the TEC magnitude of the 12-degree and 15-degree single receiver solutions approximated the reference vertical IRI diurnal values better than the 12-degree and 15-degree multiple receiver solutions. The relative good comparisons between the 12-degree and 15-degree single receiver ASHA-interpolated profiles and the reference profile is encouraging give an indication of the correct software implementation of the ASHA algorithm. The relative poor comparison of the 12-degree and 15-degree multiple receiver

solution, however, needs to be investigated as it could point to model sensitivity to receiver geometry or possible breakdown of SLM assumptions for widely distributed receivers.

The two prominent peaks present in the measured ionosonde and GPS-derived diurnal vertical TEC profiles (Fig. 4a–d) are attributed to an ionospheric travelling disturbance (McKinnell, 2006). In all the test cases, GPS-derived TEC values exceed ionosonde-derived TEC. This is as expected as the ionosonde only measures up to the F_2 peak density height (*hmF2* ~ 350 km) and the topside Chapman extrapolation (Reinisch et al., 2004) may contain some uncertainties. A significant component of the TEC difference, however, can be attributed to the plasmaspheric TEC contribution. The plasmasphere extends 1200–35,000 km above the Earth surface and contains charge densities (mostly H^+), which are considerably less than those of the ionosphere. The large extent of the plasmasphere, however, can produce significant integrated charge column densities (TEC) along signal paths passing through the plasmasphere. The daytime plasmasphere contribution to GPS-TEC is approximately ten percent, but increases to 20%–35% at night (Webb and Essex, 1997). Plasmaspheric TEC separated from GPS-TEC supplies a novel means of investigating plasmaspheric charged densities evolution and dynamics (Belehaki et al., 2004, Mazzella et al., 2002 and Belehaki and Jakowski, 2003).

In the Grahamstown comparison, the MIDAS and ASHA solutions tracked the double peak better than the GIM (Fig. 4a), and the ASHA 15-degree/single receiver solution (Fig. 4b) tracked the MIDAS solution and the second peak better and appears to be more consistent with the ionosonde data than the 12-degree/multiple receiver solution (Fig. 4a). The GIMs first peak absence might be attributed to the poor time resolution at event time. The apparent poorer performance of the 12-degree/multiple receiver ASHA solution might be attributed to the possible breakdown of the SLM spherical symmetry assumptions and should be further investigated. A higher elevation cut-off angle and different receiver configuration might improve the result.

In the Louisvale case (Fig. 4c) MIDAS and ASHA 12-degree exhibit a second peak not clearly visible in the ionosonde data and absent in the GIM data (probably due to coarse two-hour resolution). No significant difference between the 12-degree multiple receiver and 15-degree-single receiver solutions is evident.

In the Madimbo case (Fig. 4d) the 12-degree/multiple receiver and 15-degree/single receiver ASHA solutions compares well with the MIDAS solution, with the exception of the mid-day peak magnitude values and a deeper dip present in the 15-degree solution. The GIM data do

not exhibit a second peak (probably due to coarse two-hour resolution). No Madimbo ionosonde data were available for this day.

The two-dimensional TEC maps (Fig. 5) illustrate the two-hourly regional TEC variation. The estimated ASHA coefficients provide for higher spatial resolution maps at one-minute time resolution.

For near real-time applications, processing time might be significantly reduced by optimising the ASHA code, possibly re-coding in a structured programming language. It is also foreseen that the near real-time updating/downdating of the Jacobian, a computationally intensive procedure, will be faster for smaller data sets (5 min) than the 24-hour period data used in the test cases. Higher elevation cut-off angles (30°–40°) might reduce the input data set and improve processing time as well.

10. Conclusions

A regional GPS-based Ionospheric TEC model for South Africa has been developed and demonstrated. Results from this study show favourable comparisons with measured ionosonde data and two independent GPS-based methodologies. From the Grahamstown and Louisvale test cases it appears that TEC values interpolated from a 15-degree solution single receiver close to the desired interpolation point, renders a solution which appears more consistent with ionosonde observations than interpolation from a 12-degree (multiple receivers distributed across South Africa) solution. The model's sensitivity to changes in receiver geometry, model degree, elevation cut-off angles, and its performance under disturbed ionospheric conditions should be further investigated. With code optimising, a near real-time TEC mapping system for South Africa is feasible with the presented ASHA methodology.

Acknowledgements

The authors express their gratitude to Dr. Cathryn Mitchell of University of Bath, UK, for her kind assistance with the MIDAS software, to the paper reviewers for their valuable comments and to CDSM South Africa for supplying the GPS data.

References

Baumjohann, W., Treumann, R.A. (1999) Basic Space Plasma Physics. Imperial College Press. 1-86094-079-X

Belehaki, A., Jakowski, N. Comparison of ionospheric ionisation measurements over Athens using ground ionosonde and GPS-Derived TEC values (2003) Radio Science, 38 (6), p. 1105.

Belehaki, A., Jakowski, N., Reinisch, B.W. Plasmaspheric electron content derived from GPS TEC and digisonde ionograms (2004) Advances in Space Research, 33 (6), pp. 833-837.

Bilitza, D. International Reference Ionosphere 2000 (2001) Radio Science, 36 (2), pp. 261-275.

Chen, F. (1984) Introduction to Plasma Physics and Controlled Fusion. Plenum Press, 1984. 0-306-41332-9

De Franceschi, G., De Santis, A., Pau, S. Ionospheric mapping by regional Spherical Harmonic Analysis: new developments (1994) Advances in Space Research, 14 (12), pp. 61-64.

De Santis, A. Conventional spherical harmonic analysis for regional modelling of the geomagnetic field (1992) Geophysical Research Letters, 19 (10), pp. 1065-1067.

De Santis, A., De Franceschi, G., Zolesi, B., Pau, S., Cander, L.R. Regional mapping of the critical frequency of the F2 layer by spherical cap harmonic expansion (1991) Annales Geophysicae, 9, pp. 401-406.

Hargreaves, J.K. (1992) The Solar-Terrestrial Environment, Cambridge Atmospheric and Space Sciences series. Cambridge, University Press, Cambridge, UK

Hofmann-Wellenhof, B., Lichtenegger, H., Collins, J. (2001) GPS Theory and Practice. fifth ed.. Springer. 3-211-83534-2

Mazzella Jr., A.J., Holland, E.A., Andreasen, A.M., Andreasen, C.C., Rao, G.S., Bishop, G.J. Autonomous estimation of plasmasphere content using GPS measurements (2002) Radio Science, 37 (6), pp. 41-45.

Mitchell, C.N., Spencer, P.S.J. A three-dimensional time-dependent algorithm for ionospheric imaging using GPS (2003) Annals of Geophysics, 46 (4), pp. 687-696.

Reinisch, B.W., Huang, X.-Q., Belehaki, A., Shi, J.-K., Zhang, M.-L., Ilma, R. Modeling the IRI topside profile using scale heights from ground-based ionosonde measurements (2004) Advances in Space Research, 34 (9), pp. 2026-2031.

RINEX [RINEX] The Receiver Independent Exchange Format, Werner Gurtner, Astronomical Institute, University of Berne. http://pangea.stanford.edu/GP289/rinex.format.

Schaer, S. Mapping and Predicting the Earth's Ionosphere Using the Global Positioning System, PhD Dissertation, Astronomical Institute, University of Berne, Berne, Switzerland, 25 March 1999.

SPIDR [SPIDR] Space Physics Interactive Data Resource http://spidr.ru.ac.za/spidr/.

TRIGNET [TRIGNET] Trignet network of South African GPS receivers. http://www.trignet.co.za.

Webb, P.A. and Essex, E.A. (1997). A Simple model of the ionosphere plasmasphere system, in: Kulessa, A., James, G., Bateman, D., Tobar, M. (Eds.). Proceedings of the Workshop on Applications of Radio Science, WARS'97, Barossa Valley, Australia, 21–23 September 1997, pp. 190–195.